



Molecular scale insights into interaction mechanisms between organic inhibitor film and copper

Xiaocui Wu, Frédéric Wiame, Vincent Maurice, Philippe Marcus

► To cite this version:

Xiaocui Wu, Frédéric Wiame, Vincent Maurice, Philippe Marcus. Molecular scale insights into interaction mechanisms between organic inhibitor film and copper. *npj Materials Degradation*, 2021, 5 (1), pp.22. <10.1038/s41529-021-00168-3>. <hal-03212038>

HAL Id: hal-03212038

<https://hal.science/hal-03212038v1>

Submitted on 29 Apr 2021

HAL is a multi-disciplinary open access archive for the deposit and dissemination of scientific research documents, whether they are published or not. The documents may come from teaching and research institutions in France or abroad, or from public or private research centers.

L'archive ouverte pluridisciplinaire **HAL**, est destinée au dépôt et à la diffusion de documents scientifiques de niveau recherche, publiés ou non, émanant des établissements d'enseignement et de recherche français ou étrangers, des laboratoires publics ou privés.



HAL Authorization

ARTICLE OPEN



Molecular scale insights into interaction mechanisms between organic inhibitor film and copper

Xiaocui Wu¹, Frédéric Wiame¹✉, Vincent Maurice¹ and Philippe Marcus¹✉

A model experimental approach, providing molecular scale insight into the build up mechanisms of a corrosion inhibiting interface, is reported. 2-mercaptobenzimidazole (2-MBI), a widely used organic inhibitor, was deposited from the vapor phase at ultra-low pressure on copper surfaces in chemically-controlled state, and X-ray photoelectron spectroscopy was used in situ to characterize the adsorption mechanisms upon formation of the inhibiting film. On copper surfaces prepared clean in the metallic state, the intact molecules lie flat at low exposure, with sulfur and both nitrogen atoms bonded to copper. A fraction of the molecules decomposes upon adsorption, leaving atomic sulfur on copper. At higher exposure, the molecules adsorb in a tilted position with sulfur and only one nitrogen bonded to copper, leading to a densification of 2-MBI in the monolayer. A bilayer is formed at saturation with the outer layer not bonded directly to copper. In the presence of a pre-adsorbed 2D oxide, oxygen is substituted and the molecules adsorb intactly without decomposition. A 3D oxide prevents the bonding of sulfur to copper. The molecular film formed on metallic and 2D oxide pre-covered surfaces partially desorbs and decomposes at temperature above 400 °C, leading to the adsorption of atomic sulfur on copper.

npj Materials Degradation (2021)5:22; <https://doi.org/10.1038/s41529-021-00168-3>

INTRODUCTION

A study conducted by NACE in 2013 estimated the annual global cost of corrosion to about 3.4% of the global gross domestic product. It is thus of significant importance to mitigate corrosion, including for copper and its alloys which are widely used in numerous industrial applications, such as in electrical installations and electronics, in heating and cooling systems, and in building construction.

The use of organic inhibiting molecules is one of the most effective and practical ways to protect metals and alloys from corrosion in aggressive environments, hence the intrinsic properties of the molecules and their interaction mechanisms with various substrate surfaces have been studied extensively^{1–6}. Among all the techniques, X-ray photoelectron spectroscopy (XPS) has been widely used, which gives reliable information on the nature and chemical composition of the inhibitor/substrate interface under various conditions^{6–12}. The molecular chemical composition is crucial to its interaction with metal surfaces. The heteroatoms (such as sulfur, nitrogen, oxygen or phosphorus) with lone electron pair present in an organic molecule are responsible for its high corrosion inhibition efficiency by developing coordinative bonds with the metallic substrate^{7–9,11,13,14}, leading to the formation of an adhesive and protective film on the metal surface.

Benzimidazole derivatives, such as 2-mercaptobenzimidazole (2-MBI), have been widely studied as corrosion inhibitors in solution for various metals and alloys, such as steel^{15,16}, aluminum¹⁷ and copper^{1–8,11,13,14,18–20}. The molecule may exist in two tautomeric forms, as shown in Fig. 1.

In thione form, both nitrogen atoms are protonated, with sulfur double bonded to carbon. In thiol form, only one nitrogen atom is protonated and another is unprotonated. On copper surface, the molecules has been found to form a complex film through

bonding with copper, leading to the formation of a protective layer which prevents the metal from corrosion.

However, in spite of these numerous studies, the detailed interaction mechanisms of 2-MBI with copper surfaces are still discussed, and deeper insight from experimental studies at the molecular scale is needed. Notably, the form of interaction between the molecule and the substrate, whether the molecule adsorbs intactly or partially decomposes upon adsorption, and if in molecular form, the relative position of the molecule compared to the surface, i.e., whether the plane of the heterocyclic ring is parallel or perpendicular to the substrate in ‘flat-lying’ or ‘upright’ configurations, respectively. Also, the effect of the surface state, metallic or oxidized, on the bonding interaction of the molecule remains to be characterized experimentally. All these challenging questions can difficultly be answered by the traditional way of corrosion inhibition study in liquid solution. Thus, we have applied a surface science approach, innovative in the context of corrosion inhibition studies, with the deposition of high purity organic molecules by sublimation in gaseous phase under ultra-low pressure onto copper surfaces in chemically-controlled state. In this case, the thione form of the inhibitor predominates^{21,22}. Compared to the corrosion inhibition study in liquid phase, the solvent effects and air contaminations are eliminated, allowing a more fundamental study of the molecule/substrate interactions governing the build up of the inhibiting interface, thus offering a rational basis for the better understanding of the corrosion inhibition mechanisms in real conditions.

Combining Auger electron spectroscopy (AES), scanning tunneling microscopy (STM) and ex situ XPS analysis on (111)-oriented copper single-crystal surfaces, it was shown that a self-assembled monolayer is formed at low exposure, and a fraction of molecules decompose, leading to the adsorption of atomic sulfur on copper²³. Using density functional theory (DFT) modeling, the

¹Université PSL, CNRS - Chimie ParisTech, Institut de Recherche de ChimieParis, Physical Chemistry of Surfaces Group, Paris, France. ✉email: frederic.wiame@chimieparistech.psl.eu, philippe.marcus@chimieparistech.psl.eu

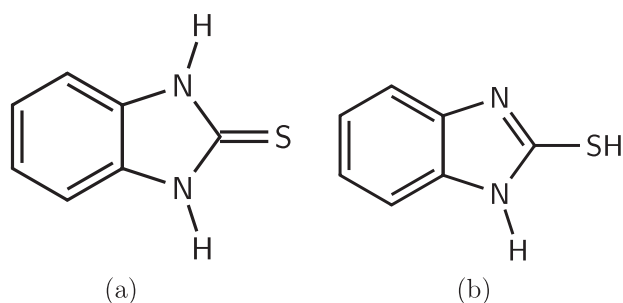


Fig. 1 Conformations of the 2-MBI molecule. **a** Thione form and **b** thiol form.

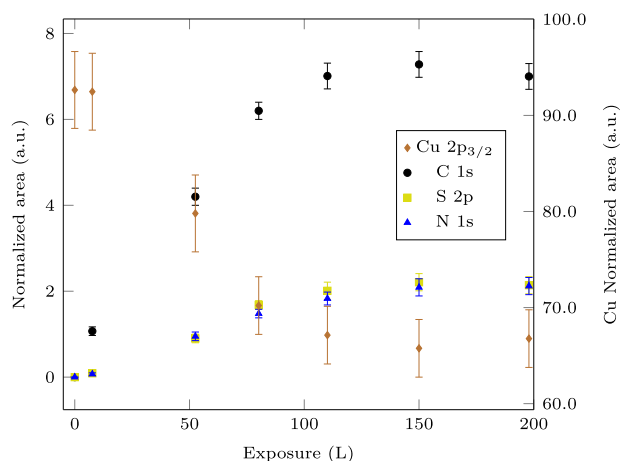


Fig. 2 Growth kinetics of 2-MBI at RT on the metallic Cu(111) surface. Evolution of the Cu 2p_{3/2}, C 1s, S 2p and N 1s normalized areas with 2-MBI exposure. The error bars were estimated by adjusting the fit of the XPS core levels.

most stable adsorbed configuration was found for the thiolate form with sulfur and nitrogen bonded to copper¹⁸.

In the present work, we applied XPS *in situ* to study the growth and the nature of the chemical interaction of the adsorbed molecular layer on a Cu(111) single crystal, thus avoiding the influence of grain boundaries and dissimilar grain orientations. Adsorption of 2-MBI was carried out by direct sublimation under ultra-high vacuum (UHV) conditions onto surfaces in well-controlled metallic or pre-oxidized state. The influence of a surface oxide on the adsorption of molecules was investigated by vapor sublimation of the molecule to pre-oxidized copper surfaces. The thermal stability of the adsorbed molecular layer was also studied. Finally, the results were compared to those obtained with another structurally related inhibitor, 2-mercaptobenzothiazole (2-MBT), that we studied previously^{24,25}.

RESULTS AND DISCUSSION

2-MBI growth on metallic copper

Figure 2 shows the growth kinetics of 2-MBI deposited at RT on the copper surface prepared clean in the metallic state and followed by XPS. The areas of the Cu 2p_{3/2}, C 1s, S 2p and N 1s spectra were measured and normalized by the transmission of the analyzer, the photoionization cross section of each element and the corresponding inelastic mean free path. The normalized area is thus proportional to the atomic density of each element, and is plotted as a function of 2-MBI exposure.

The intensities of C 1s, S 2p and N 1s core levels increase with increasing exposure, accompanied by a decrease of Cu 2p_{3/2} intensity, showing the growth of the adsorbed molecular layer on

the Cu(111) surface, leading to the attenuation of the metallic substrate. The adsorption rate decreases gradually with increasing exposure, until reaching a saturation regime. The N to C atomic ratio was calculated to be close to that for the stoichiometry of 2-MBI (2/7), confirming the adsorption of 2-MBI molecules. An excess of S is clearly observed, with the S to C atomic ratio about two times the value corresponding to the stoichiometry (1/7). This is consistent with the AES measurement showing the adsorption of 2-MBI with an excess of sulfur²³.

The origin of this excess of sulfur is studied further by a thorough analysis of the high resolution XPS spectra obtained on the metallic Cu(111) after different exposures to 2-MBI at ultra-low pressure and RT, as shown in Fig. 3. Two spin-orbit doublets, S 2p_{1/2} and S 2p_{3/2}, of branching ratio of 1:2 and of spin-orbit splitting of 1.18 eV were used to decompose the S 2p spectra^{26,27}. At 8 L, only a S₂ component is observed, with the 2p_{3/2} peak at binding energy of 161.4 eV. This component was also observed on Cu(111) exposed to 2-MBT and to 2-MBI, and was assigned to sulfur bonded to copper^{23,24}. Moreover, S₂ is located at the same binding energy as the S 2p spectrum observed on Cu(111) with adsorbed atomic sulfur obtained by exposing to H₂S²⁴. So there might be a partial decomposition of 2-MBI by the cleavage of the C=S bond and the adsorption of both atomic sulfur and intact molecules on copper, while the molecular fragments resulting from the partial decomposition leave the surface. This is in good agreement with the coexistence of the ($\sqrt{7} \times \sqrt{7}$)R19.1° structure formed by atomic sulfur and the (8 × 8) structure formed by the intact molecule in the monolayer as suggested by STM²³, and could also explain the excess of sulfur discussed above. Meanwhile, a second component S₁ is observed at a 2p_{3/2} binding energy of 162.3 eV, with a relative proportion of 24%, corresponding to sulfur in the 2-MBI molecule not interacting with copper^{9,11,23}. The presence of S₁ suggests the beginning of the formation of a second molecular layer, which is in good agreement with the completion of a monolayer at 5 L as observed by STM²³. The N 1s spectrum is composed of a unique component N₂ at a binding energy of 398.7 eV, which could be assigned to nitrogen bonded to copper, most probably in protonated form⁹. The bonding of both sulfur and the two nitrogen atoms to copper indicates that the molecules in the monolayer lie flat on the surface.

At higher exposure, the relative proportion of S₁ increases, indicating the continuous growth of 2-MBI beyond the monolayer, with the additional molecules not bonded to the Cu(111) via the S atom, as also observed by STM²³. At the same time, the intensity of S₂ increases as well, suggesting a reorganization of the molecules in the monolayer bonded to Cu(111) via the S atoms, which can be explained by a densification of the monolayer enabled by a tilt of the molecules. The densification of the monolayer directly bonded to Cu(111) is supported by the increasing intensity of N₂ until saturation. With increasing exposure, a second component N₁ appears at a binding energy varying from 399.8 eV to 400.5 eV, which could be assigned to nitrogen not bonded to copper¹¹. The high intensity of N₁ and N₂ at saturation is consistent with a reorientation of the molecule in the monolayer, leading to the adsorption of 2-MBI in a tilted position with only one nitrogen atom bonded to copper in addition to the adsorption of 2-MBI in the upper molecular layer not interacting with copper. The bonding of one nitrogen atom to copper changes the electron environment of the other nitrogen atom. The change in the relative proportion of 2-MBI with one nitrogen bonded to copper compared to that with both nitrogen atoms not interacting with copper could explain the shift in the binding energy of N₁ with increasing exposure. The atomic ratio of S₂ to N₂ was calculated, and was found to be superior to 1 (1.1–1.4) at different exposures. Compared to the stoichiometric ratio in the molecule (1/2), the high S₂ to N₂ ratio confirms the partial decomposition of the molecule upon build up of the

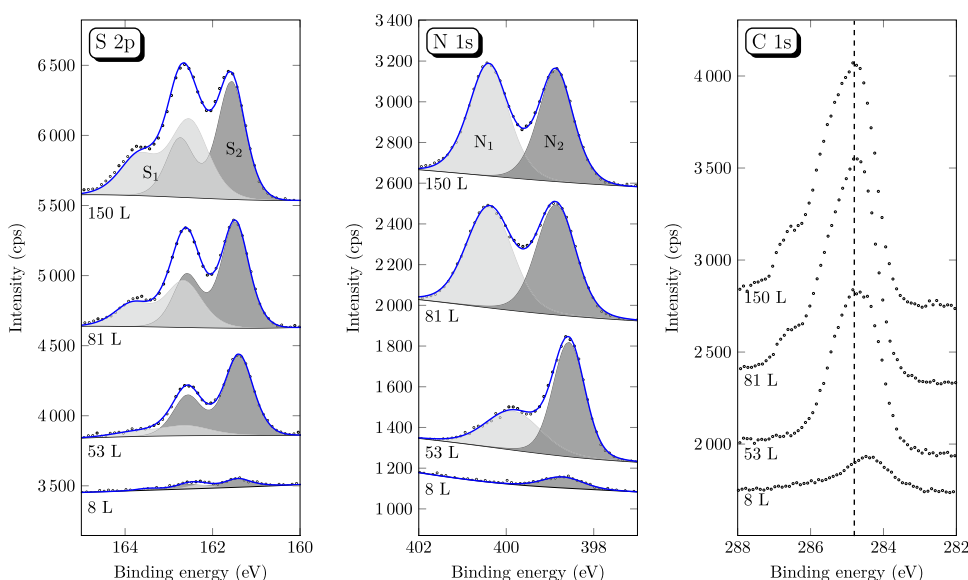


Fig. 3 High resolution XPS spectra obtained after 2-MBI exposure on the metallic Cu(111) surface at ultra-low pressure and RT. The S 2p, N 1s and C 1s core levels.

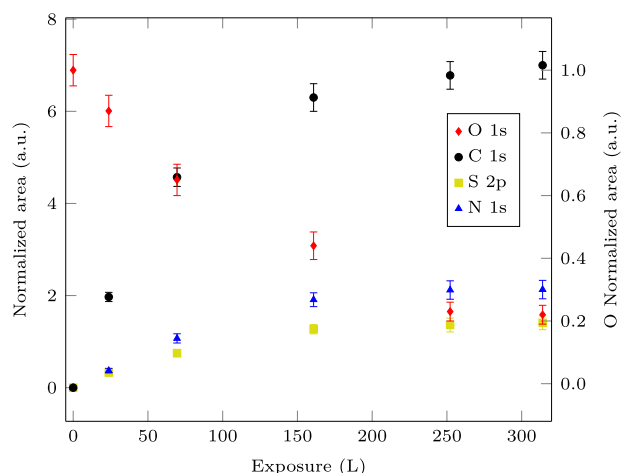


Fig. 4 Growth kinetics of 2-MBI at RT on the pre-oxidized Cu(111) (2D oxide). Evolution of the C 1s, S 2p, N 1s and O 1s normalized areas with 2-MBI exposure. The error bars were estimated by adjusting the fit of the XPS core levels.

adsorbed multilayer. The decomposition of 2-MBT was also observed on the metallic Cu(111) surface, but the molecules in the monolayer remained to lie flat with increasing exposure²⁴. Densification of the 2-MBI monolayer, with tilted molecules bonded to copper by the sulfur atom and one nitrogen atom, is in agreement with DFT calculations showing that such a bonding configuration is favored at high coverage and allows the formation of self-assembled monolayers¹⁸.

2-MBI deposition on pre-oxidized copper

The influence of surface pre-oxidation on the adsorption of 2-MBI was also investigated. To this end, a 2D surface oxide was prepared at low oxygen pressure as described in the Methods section, and the growth kinetics of 2-MBI on this pre-oxidized Cu (111) surface at RT was followed by XPS, as shown in Fig. 4. The areas of C 1s, S 2p and N 1s signals were normalized to be proportional to their atomic densities. The area of the O 1s signal was normalized by that measured on Cu(111) with a complete 2D oxide layer before 2-MBI exposure.

The adsorption of molecules on Cu(111) with pre-covered 2D oxide layer was evidenced by a rapid increase in C 1s, S 2p and N 1s intensities, accompanied by a decrease of the adsorption rate, until a saturation regime is reached. The N to C atomic ratio was found to be close to the stoichiometric value in the molecule, confirming the adsorption of 2-MBI on the pre-oxidized Cu(111). An excess of sulfur was observed, but with a S to C atomic ratio lower than that obtained on metallic Cu(111) exposed to 2-MBI, confirming AES measurements²³.

Meanwhile, the intensity of oxygen decreases continuously with increasing 2-MBI exposure, with a residual oxygen intensity representing 22% of that measured on the initial 2D oxide layer, after an exposure of 250 L. There are two possibilities to explain this decrease in oxygen intensity: the attenuation of the oxygen signal by the upper adsorbed molecular layer or the substitution of oxygen by 2-MBI at RT. A similar phenomenon has been observed for 2-MBT and for H₂S molecules^{25,28}, and the complete substitution of oxygen was evidenced after a 2-MBT exposure of only 25 L.

A detailed high resolution XPS analysis of the 2-MBI film formed on the pre-oxidized Cu(111) surface with 2D oxide layer after different exposures was performed. Figure 5 shows the high resolution XPS spectra of the S 2p, N 1s and O 1s core levels obtained after different 2-MBI exposures at RT. The S 2p spectra show the presence of two components S₁ and S₂, with the 2p_{3/2} peaks at 162.5 eV and 161.5 eV, corresponding to sulfur not bonded and bonded to Cu, respectively. The molecules adsorb in the monolayer on copper via bonding with sulfur. With increasing exposure, adsorption of 2-MBI in the molecular monolayer occurs, and the additional molecules do not bond directly to copper via the sulfur atom, giving a S₁ component whose intensity increases rapidly with increasing exposure. Moreover, the intensity of S₂ is about three times lower than that measured on the metallic Cu (111) surface, indicating a lower density of interface sulfur interacting with copper, which suggests that the molecules adsorb mainly in their intact form in the monolayer. The N 1s spectra show a unique component N₂ at binding energy of 398.5 eV at low exposure, indicating that both nitrogen atoms are bonded to copper on the pre-oxidized sample surface. This component is shifted to lower binding energy (0.2 eV) compared to that measured on the metallic Cu(111) surface, which could be explained by the modification of the structure of the copper substrate resulting from the oxidation process prior to exposure of

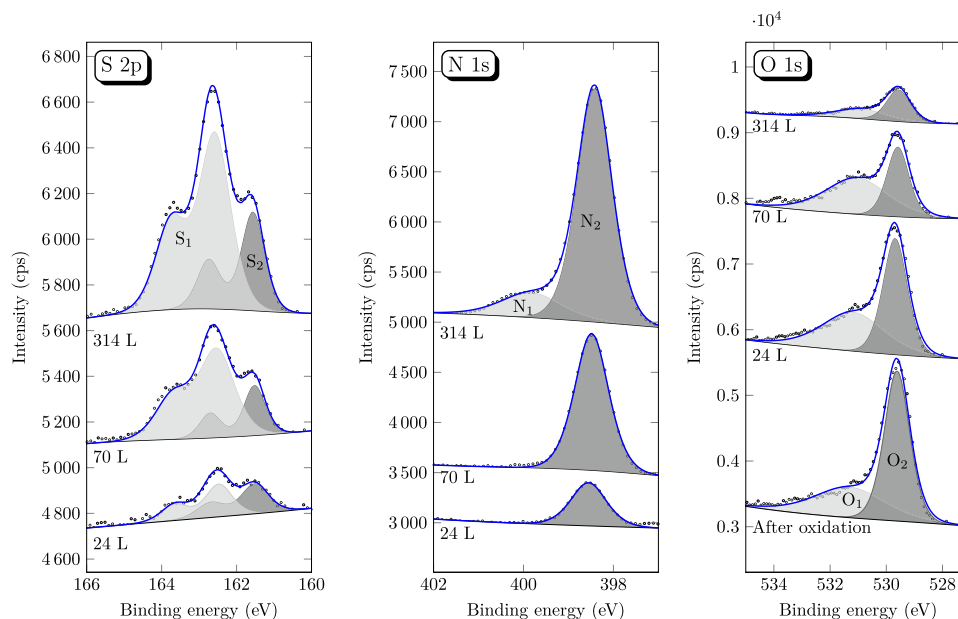


Fig. 5 High resolution XPS spectra obtained after 2-MBI exposure on pre-oxidized Cu(111) surface (2D oxide) at ultra-low pressure and RT. The S 2p, N 1s and O 1s core levels.

2-MBI. The atomic ratio of S_2 to N_2 was calculated to be about 0.4 at low exposure, which is close to the stoichiometric value in the molecule, confirming the adsorption of intact molecules without decomposition of 2-MBI. The adsorption of 2-MBT on pre-oxidized Cu(111) surface was studied, the molecules adsorb intactly to copper through bonding with sulfur without decomposition²⁴.

As for the decomposition of the O 1s spectra, two components O_1 and O_2 are observed at binding energies of 531.1 eV and 529.6 eV, with a full width at half-maximum (FWHM) of 1.0 eV and 2.5 eV, respectively. According to previous studies on the “29” structure formed in these pre-oxidation conditions^{29,30}, atomically accurate models were proposed with oxygen adsorbed in two different environments: O anions in Cu-O hexagonal ring and O adatom in the center of the ring. The component O_2 at lower binding energy is usually attributed to the bulk oxide^{31,32}, which could in this case be assigned to O anion bonded to copper in the hexagonal ring. O_1 component at higher binding energy may then be attributed to O adatom. The decrease of the oxygen intensity is mainly due to the decrease of O_2 component, indicating the substitution of oxygen in copper oxide by the 2-MBI molecule, and the normalized area in Fig. 4 represents then the fraction of surface covered by oxygen.

In order to simulate the adsorption mode of 2-MBI on Cu(111) pre-oxidized in more realistic conditions, the clean metallic Cu (111) surface prepared under UHV was exposed firstly to air at RT. In this case, a 3D oxide was formed on Cu(111). The sample was then introduced into the UHV system for the deposition of molecules under ultra-low pressure at RT. XPS analysis before deposition of 2-MBI indicates that the so-formed 3D oxide consists of a mixture of Cu_2O and CuO, as shown in the Cu LMM Auger spectrum in Fig. 6, with a thickness of about 1.1 nm. The presence of carbon contaminations is also detected. The high resolution XPS spectra of the Cu LMM, S 2p, N 1s and C 1s core levels are also shown in Fig. 6 after exposure at RT to 2-MBI until saturation. The intensity of Cu LMM spectrum decreases by 11%, which can be explained by the attenuation of the substrate by the molecules. Also the relative proportion of CuO and Cu decreases, while that of Cu_2O increases slightly.

On the Cu(111) surface with this 3D oxide, only the S_1 component is observed after 2-MBI exposure, indicating that the 3D oxide layer prevents the decomposition of the molecules and

that the adsorbed molecules do not bond via the S atoms to copper of the surface oxide. Nitrogen is bonded to copper in the 3D oxide, as confirmed by the high intensity N_2 component. The S to N atomic ratio was calculated to be about 0.6, confirming the adsorption of intact molecule without decomposition of 2-MBI. Moreover, the decomposition of C 1s spectrum was performed. Since XPS may not distinguish between the four carbon atoms in the benzene ring not in direct contact with N^{9,33}, we assume three different types of carbon environments, with the same FWHM and a intensity ratio of 1:2:4. A good fit was obtained, with C_1 , C_2 and C_3 at binding energies of 285.9 eV, 284.9 eV and 284.2 eV, corresponding to C=S, C=N, and the remaining C atoms in the benzene ring, respectively. This confirms the adsorption of the intact molecule on the 3D oxide pre-covered Cu(111) surface. DFT calculation confirms the strong interaction of the molecules with copper oxide through bonding with sulfur and nitrogen³⁴. Based on the above analysis, Fig. 7 shows a schematic illustration of the adsorption of 2-MBI on metallic and pre-oxidized Cu(111) surfaces.

Thickness of 2-MBI layer on metallic copper

Since XPS is a quantitative technique, the thickness of the 2-MBI film formed on the metallic Cu(111) surface was calculated. To this end, we assume that the molecular layer is homogeneous and continuous on Cu(111). The thickness of the inhibitor layer was then calculated using the following equations:

$$I_{S2p}^{MBI} = kFSN_S^{MBI}\sigma_{S2p}T_{S2p}\lambda_{S2p}^{MBI}\sin\theta\left[1 - \exp\left(-\frac{d_{MBI}}{\lambda_{S2p}^{MBI}\sin\theta}\right)\right] \quad (1)$$

$$I_{N1s}^{MBI} = kFSN_N^{MBI}\sigma_{N1s}T_{N1s}\lambda_{N1s}^{MBI}\sin\theta\left[1 - \exp\left(-\frac{d_{MBI}}{\lambda_{N1s}^{MBI}\sin\theta}\right)\right] \quad (2)$$

$$I_{Cu}^{Cu} = kFSN_{Cu}^{Cu}\sigma_{Cu2p}T_{Cu2p}\lambda_{Cu2p}^{Cu}\sin\theta\exp\left(-\frac{d_{MBI}}{\lambda_{Cu2p}^{Cu}\sin\theta}\right) \quad (3)$$

where k is a constant which is characteristic of the spectrometer used, F the photon flux (constant), S the area of the analyzed zone, I is the intensity of the photoelectrons, N the density of the emitting atoms, σ the photoionization cross section, T the transmission of the analyzer, λ the inelastic mean free path of

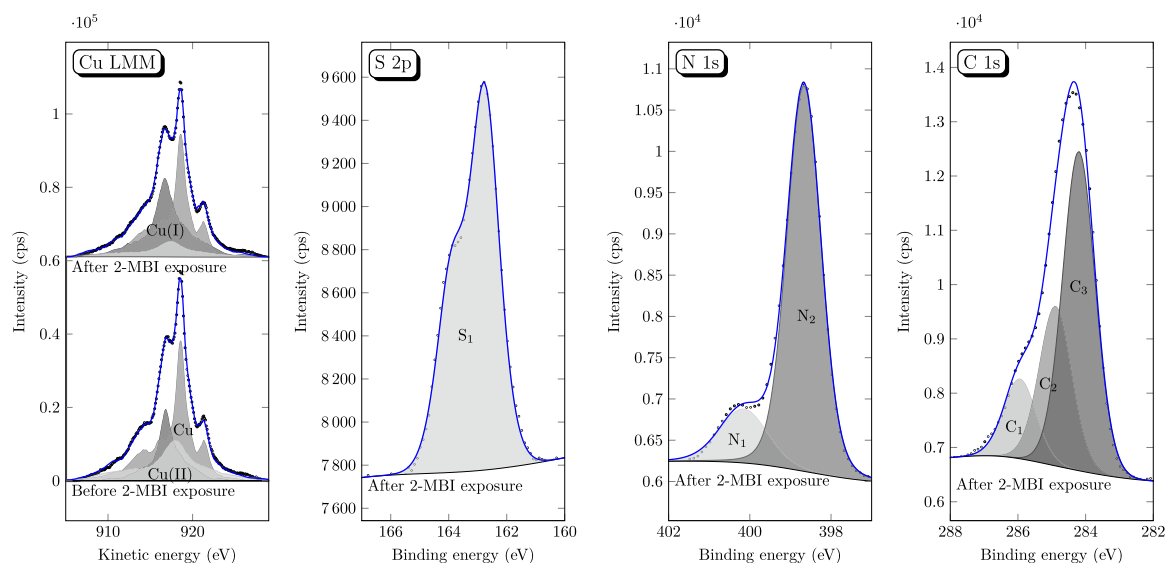


Fig. 6 High resolution XPS spectra obtained before and after 2-MBI exposure until saturation on Cu(111) pre-exposed to air (3D oxide) at 1×10^{-9} mbar of 2-MBI and RT. The Cu LMM Auger spectra before and after 2-MBI exposure and S 2p, N 1s and C 1s core levels after 2-MBI exposure.

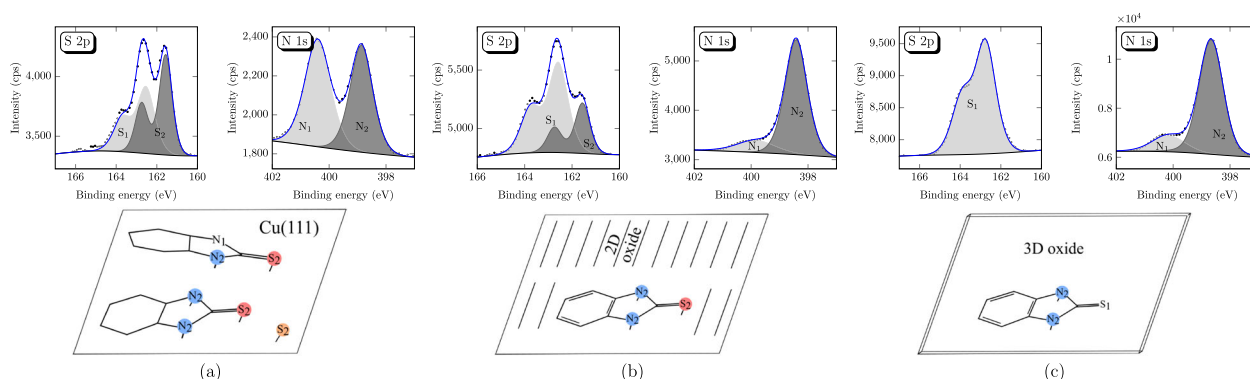


Fig. 7 Schema of 2-MBI adsorption on copper surfaces and the corresponding S 2p and N 1s spectra. **a** Metallic; **b** oxidized (2D oxide); **c** oxidized (3D oxide).

emitted electrons, which is estimated by the Tanuma, Powell and Penn formula (TPP-2M)³⁵, θ the take-off angle of the photoelectrons, and d_{MBI} the thickness of the 2-MBI layer.

The thickness of the molecular layer increases with increasing exposure, as shown in Fig. 8. At 8 L, XPS analysis indicates the formation of a complete monolayer of 2-MBI as discussed above, and the thickness of the inhibitor film is about 0.1 ± 0.1 nm. This is consistent with the thickness calculated in the literature for a single 2-MBI monolayer⁹. Taking into account the size of the 2-MBI molecule of $7.9 \text{ \AA} \times 9.7 \text{ \AA}$ in the molecular plane²², the molecules are very likely to lie flat, which is in good agreement with the XPS analysis indicating bonding via sulfur and both nitrogen atoms to copper. Moreover, STM²³ indicates the formation of a second layer at 11 L. The continuous increase of the film thickness after 11 L could be explained by the change in the molecule configuration as evidenced by our XPS analysis above. At saturation, the thickness of the 2-MBI film is about 0.8 nm, which could be explained by the adsorption of two molecular layers. The 2-MBI film formed at saturation is thicker than that formed by 2-MBT (0.6 nm), which could be explained by the change in the 2-MBI configuration from flat-lying to tilted geometry with increasing exposure.

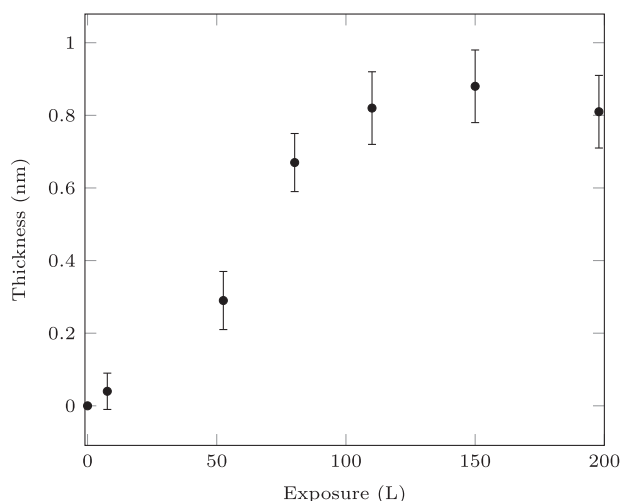


Fig. 8 Thickness of the 2-MBI film formed on the metallic Cu(111) surface. The error bars were estimated by taking into account the errors of all the parameters used for calculation.

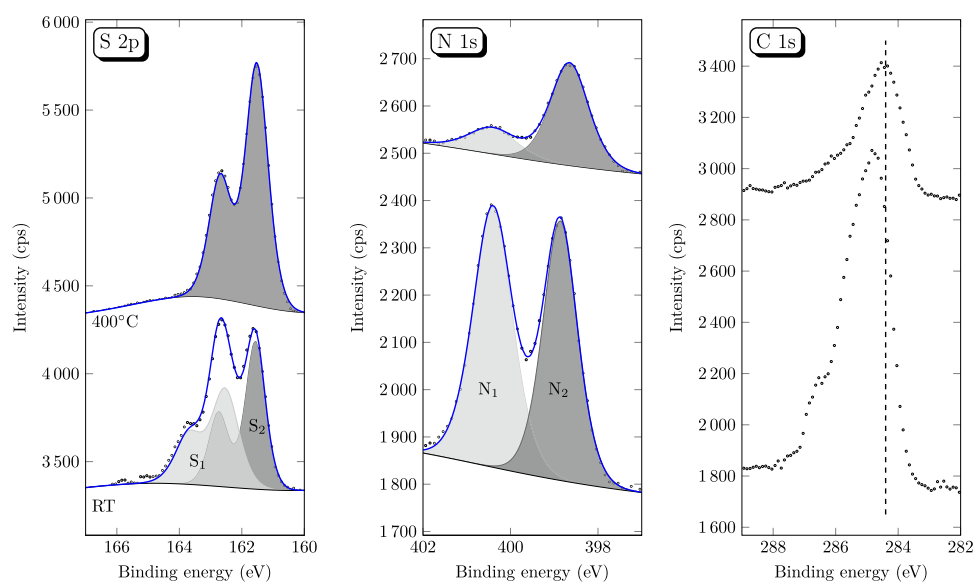


Fig. 9 High resolution XPS spectra obtained on the metallic Cu(111) with pre-adsorbed 2-MBI layer at saturation before and after annealing at 400 °C during 10 min. The S 2p, N 1s and C 1s core levels.

Thermal stability of the 2-MBI molecular layer

In order to study the thermal stability of the 2-MBI layer, the metallic Cu(111) surface with pre-covered 2-MBI at saturation was annealed at different temperatures, and the surface after annealing was analyzed by XPS, as shown in Fig. 9.

A clear change in the surface composition was observed after annealing above 400 °C (no change for annealing below 400 °C). For the S 2p spectra, the S_1 component disappears after annealing, suggesting a desorption of the 2-MBI molecules in the upper layer, as also confirmed by the rapid decrease of N 1s (especially the N_1 component) and C 1s intensities. Meanwhile, the intensity of the S_2 component increases to 1.7 times that before annealing, and the S to C atomic ratio was calculated to be about six times the stoichiometric value (1/7). This indicates a further decomposition of the molecule after annealing and the adsorption of atomic sulfur on copper. The results are in good agreement with STM characterization showing the formation of an ordered layer with $(\sqrt{7} \times \sqrt{7})R19.1^\circ$ structure after annealing at 500 °C²³. The same experiment was performed to investigate the thermal stability of 2-MBI layer formed on pre-oxidized Cu(111) (2D oxide) at saturation, a desorption and further decomposition of the molecules were also observed when annealing above 500 °C. Compared to the 2-MBT molecular layer which decomposes after annealing above 100 °C²⁴, a higher thermal stability was evidenced for 2-MBI, which could be explained by its higher adsorption energy compared to that of 2-MBT as indicated by DFT calculation¹⁸.

To summarize, this model surface science approach, combining adsorption of organic molecules at ultra-low pressure onto chemically-controlled metal surfaces with in situ surface analysis, exemplifies how deeper experimental insight on inhibition mechanisms can be obtained. Applied in the present work to 2-MBI deposited on copper and analyzed by high resolution XPS, it provides molecular scale insight on the interfacial interaction mechanisms leading to the formation of an inhibitor film.

On the metallic copper surface, an excess of sulfur was observed in the molecular film. A S_2 component at binding energy of 161.4 eV characterized sulfur bonded to copper, both in the intact molecule and in atomic form resulting from the decomposition of 2-MBI. Initially, both sulfur and two nitrogen were bonded to copper, indicating that the molecule was lying flat on copper. With increasing exposure, a densification of the

monolayer directly bonded to copper was observed, accompanied by a reorientation of the molecule to a tilted configuration. In this case, only one nitrogen atom remained bonded to copper. Quantitative calculation indicated that the thickness of the molecular layer formed at saturation was about 0.8 nm, suggesting the formation of a bilayer with the inner molecular layer directly bonded to copper and the outer layer not bonded to copper.

On copper pre-covered with a 2D oxide layer, dissociation of the surface oxide and substitution of oxygen by the molecules was observed, without decomposition of the molecule. Both sulfur and the two nitrogen atoms were bonded to copper, suggesting flat-lying molecules on copper. In the presence of a 3D oxide, only bonding between nitrogen and copper was observed, indicating a weaker interaction of 2-MBI with the oxidized surface.

Partial desorption and decomposition of the 2-MBI film pre-adsorbed on metallic copper was observed above 400 °C. The 2-MBI molecular layer formed on copper has a higher thermal stability in comparison to that formed by 2-MBT.

METHODS

System and characterization techniques

Experiments were performed in an ESCALAB 250 photoelectron spectrometer purchased from Thermo Electron Corporation. The system was pumped continuously in order to keep a base pressure below 10^{-10} mbar. XPS analysis was performed using a monochromatic Al K_α X-ray source (1486.6 eV). The binding energy was calibrated by referring to the Fermi level of the sample. Reference samples were used to calibrate the transmission of the analyzer. The high resolution core level spectra were recorded with a pass energy of 20 eV, which corresponds to an overall resolution of 360 meV. The analyzed photoelectrons were collected with a take-off angle of 90°, and the XPS spectra were analyzed using the CasaXPS software (version 2.3.19)³⁶.

Materials and sample preparation

The sample used was a high purity (99.999%) Cu(111) single-crystal. A clean Cu(111) surface was prepared by repeated cycles of ion sputtering ($P_{Ar} = 5 \times 10^{-6}$ mbar, 600 V, 10 mA, 10 min) and annealing to 600 °C during 10 min. The surface was systematically checked until no contamination was observed in the XPS survey spectrum, and a sharp (1×1) low energy electron diffraction pattern was obtained. Pre-oxidation of the Cu(111) surface was performed by introducing oxygen gas in the preparation chamber ($P_{O_2} = 5 \times 10^{-6}$ mbar) until saturation (15 min). In these

conditions, a 2D surface oxide with “29” superstructure was formed^{29,30,37}. A 3D oxide was also prepared by exposing the metallic Cu(111) surface to air.

2-MBI deposition

A vacuum sealed glass tube containing 2-MBI powder was connected to the UHV preparation chamber of the spectrometer for the in situ deposition of the molecules. The above prepared Cu(111) surfaces were transferred to the preparation chamber connected to the vacuum sealed glass tube for 2-MBI exposure. 2-MBI powder, purchased from Sigma-Aldrich, has a purity higher than 98%. The pressure in the tube and preparation chamber was in the order of 10^{-9} mbar during exposure at room temperature (RT). The sample was kept at RT during the deposition process, and the growth kinetics of 2-MBI was followed by XPS. The molecular exposure is expressed in langmuir ($1 \text{ L} = 10^{-6} \text{ torr s}$).

DATA AVAILABILITY

The data that support the findings of this study are available from the corresponding authors upon reasonable request.

Received: 14 January 2021; Accepted: 22 March 2021;

Published online: 28 April 2021

REFERENCES

- Putilova, N., Balezin, S. & Barannik, V. *Metallic Corrosion Inhibitors*. (Pergamon Press, 1966).
- Al Kharafi, F., Al-Awadi, N., Ghayad, I., Abdullah, R. & Ibrahim, M. Novel technique for the application of azole corrosion inhibitors on copper surface. *Mater. Trans.* **51**, 1671–1676 (2010).
- Gece, G. Drugs: A review of promising novel corrosion inhibitors. *Corros. Sci.* **53**, 3873–3898 (2011).
- Petrović Mihajlović, M. & Antonijević, M. Copper corrosion inhibitors. Period 2008–2014. A review. *Int. J. Electrochem. Sci.* **10**, 1027–1053 (2015).
- Costa, D. & Marcus, P. Adsorption of organic inhibitor molecules on metal and oxidized surfaces studied by atomic theoretical methods. In Taylor, C. D. & Marcus, P. (eds.) *Molecular modeling of corrosion processes: scientific development and engineering applications, first edition*, 125–156 (John Wiley & Sons, Inc., 2015).
- Fateh, A., Aliofkhaizraei, M. & Rezvanian, A. Review of corrosive environments for copper and its corrosion inhibitors. *Arab. J. Chem.* **13**, 481–544 (2020).
- Chadwick, D. & Hashemi, T. Electron spectroscopy of corrosion inhibitors: Surface film formed by 2-mercaptobenzothiazole and 2-mercaptobenzimidazole on copper. *Surf. Sci.* **89**, 649–659 (1979).
- Xue, G., Huang, X.-Y., Dong, J. & Zhang, J. The formation of an effective anti-corrosion film on copper surfaces from 2-mercaptobenzimidazole solution. *J. Electroanal. Chem.* **310**, 139–148 (1991).
- Whelan, C. M., Smyth, M. R., Barnes, C. J., Brown, N. M. D. & Anderson, C. A. An XPS study of heterocyclic thiol self-assembly on Au (111). *Appl. Surf. Sci.* **134**, 144–158 (1998).
- Gašparac, R., Martin, C. R., Stupnišek-Lisac, E. & Mandić, Z. In situ and ex situ studies of imidazole and its derivatives as copper corrosion inhibitors. II. AC impedance, XPS, and SIMS studies. *J. Electrochem. Soc.* **147**, 991 (2000).
- Finšgar, M. 2-mercaptobenzimidazole as a copper corrosion inhibitor: Part II. Surface analysis using X-ray photoelectron spectroscopy. *Corros. Sci.* **72**, 90–98 (2013).
- Kuznetsov, Y. I. Organic corrosion inhibitors: where are we now? part I. Adsorption. *Int. J. Corros. Scale Inhib.* **4**, 284–310 (2015).
- Trachli, B., Keddama, M., Takenouti, H. & Sghiri, A. Protective effect of electro-polymerized 2-mercaptobenzimidazole upon copper corrosion. *Prog. Org. Coat.* **44**, 17–23 (2002).
- Sun, S. et al. Density functional theory study of imidazole, benzimidazole and 2-mercaptobenzimidazole adsorption onto clean Cu(111) surface. *Corros. Sci.* **63**, 140–147 (2012).
- Farjami, A., Yousefina, H., Seydroufi, Z.-S. & Shajari, Y. Investigation of inhibitive effects of 2-mercaptobenzimidazole (2-MBI) and polyethyleneimine (PEI) on pitting corrosion of austenitic stainless steel. *J. Bio-and Tribo-Corrosion* **6**, 1–19 (2020).
- Lgaz, H. et al. Evaluation of 2-mercaptobenzimidazole derivatives as corrosion inhibitors for mild steel in hydrochloric acid. *Met.* **10**, 357 (2020).
- Obot, I., Gasem, Z. & Umoren, S. Understanding the mechanism of 2-mercaptobenzimidazole adsorption on Fe (110), Cu (111) and Al (111) surfaces: DFT and molecular dynamics simulations approaches. *Int. J. Electrochem. Sci.* **9**, 2367–2378 (2014).
- Vernack, E., Costa, D., Tingaut, P. & Marcus, P. DFT studies of 2-mercaptobenzothiazole and 2-mercaptobenzimidazole as corrosion inhibitors for copper. *Corros. Sci.* **174**, 108840 (2020).
- Huang, H. & Bu, F. Correlations between the inhibition performances and the inhibitor structures of some azoles on the galvanic corrosion of copper coupled with silver in artificial seawater. *Corros. Sci.* **165**, 108413 (2020).
- Sisso, O., Dor, S., Eliyahu, D., Sabatani, E. & Eliaz, N. Corrosion inhibition of copper in ferric chloride solutions with organic inhibitors. *npj Mater. Degrad.* **4**, 1–16 (2020).
- Silva, A. L. R. & da Silva, M. D. M. C. R. Energetic, structural and tautomeric analysis of 2-mercaptobenzimidazole. *J. Therm. Anal. Calorim.* **129**, 1679–1688 (2017).
- Form, G., Raper, E. & Downie, T. The crystal and molecular structure of 2-mercaptobenzimidazole. *Acta Crystallogr. B Struct. Cryst. Cryst. Chem.* **32**, 345–348 (1976).
- Wu, X., Wiame, F., Maurice, V. & Marcus, P. 2-mercaptobenzimidazole films formed at ultra-low pressure on copper: adsorption, thermal stability and corrosion inhibition performance. *Appl. Surf. Sci.* **527**, 146814 (2020).
- Wu, X., Wiame, F., Maurice, V. & Marcus, P. 2-mercaptobenzothiazole corrosion inhibitor deposited at ultra-low pressure on model copper surfaces. *Corros. Sci.* **166**, 108464 (2020).
- Wu, X., Wiame, F., Maurice, V. & Marcus, P. Adsorption and thermal stability of 2-mercaptobenzothiazole corrosion inhibitor on metallic and pre-oxidized Cu (111) model surfaces. *Appl. Surf. Sci.* **508**, 145132 (2020).
- Jia, J. et al. On sulfur core level binding energies in thiol self-assembly and alternative adsorption sites: An experimental and theoretical study. *J. Chem. Phys.* **143**, 104702 (2015).
- Finšgar, M. & Merl, D. K. An electrochemical, long-term immersion, and XPS study of 2-mercaptobenzothiazole as a copper corrosion inhibitor in chloride solution. *Corros. Sci.* **83**, 64–175 (2014).
- Wiame, F., Maurice, V. & Marcus, P. Reactivity to sulphur of clean and pre-oxidized Cu(111) surfaces. *Surf. Sci.* **600**, 3540–3543 (2006).
- Matsumoto, T. et al. Scanning tunneling microscopy studies of oxygen adsorption on Cu(111). *Surf. Sci.* **471**, 225–245 (2001).
- Therrien, A. J. et al. Structurally accurate model for the “29”-structure of $\text{Cu}_x\text{O}/\text{Cu}$ (111): a DFT and STM study. *J. Phys. Chem. C* **120**, 10879–10886 (2016).
- Kautek, W. & Gordon II, J. G. XPS studies of anodic surface films on copper electrodes. *J. Electrochem. Soc.* **137**, 2672 (1990).
- Wiame, F. et al. Oxidation of α -brass: a photoelectron spectroscopy study. *Surf. Sci.* **641**, 51–59 (2015).
- Whelan, C. M., Smyth, M. R. & Barnes, C. J. HREELS, XPS, and electrochemical study of benzenethiol adsorption on Au(111). *Langmuir* **15**, 116–126 (1999).
- Chiter, F., Costa, D., Maurice, V. & Marcus, P. Adsorption of 2-mercaptobenzimidazole corrosion inhibitor on copper: DFT study on model oxidized interfaces. *J. Electrochem. Soc.* **167**, 161506 (2020).
- Tanuma, S., Powell, C. J. & Penn, D. R. Calculations of electron inelastic mean free paths. IX. Data for 41 elemental solids over the 50 eV to 30 keV range. *Surf. Interfac. Anal.* **43**, 689–713 (2011).
- Casaxps manual 2.3.15. Casa Software Ltd (2009). <http://www.casaxps.com>.
- Wiame, F., Maurice, V. & Marcus, P. Initial stages of oxidation of Cu(111). *Surf. Sci.* **601**, 1193–1204 (2007).

ACKNOWLEDGEMENTS

This project has received funding from the European Research Council (ERC) under the European Union's Horizon 2020 research and innovation program (ERC Advanced Grant CIMNAS no. 741123).

AUTHOR CONTRIBUTIONS

The study was conceived by F.W., V.M. and P.M., X.W. performed surface preparation, all experiments and data acquisition as well as analysis under the supervision of F.W. All authors discussed the data interpretation. X.W. wrote the paper first draft, revised by F.W., V.M. and P.M. All authors approved the final version.

COMPETING INTERESTS

The authors declare no competing interests.

ADDITIONAL INFORMATION

Correspondence and requests for materials should be addressed to F.W. or P.M.

Reprints and permission information is available at <http://www.nature.com/reprints>

Publisher's note Springer Nature remains neutral with regard to jurisdictional claims in published maps and institutional affiliations.



Open Access This article is licensed under a Creative Commons Attribution 4.0 International License, which permits use, sharing,

adaptation, distribution and reproduction in any medium or format, as long as you give appropriate credit to the original author(s) and the source, provide a link to the Creative Commons license, and indicate if changes were made. The images or other third party material in this article are included in the article's Creative Commons license, unless indicated otherwise in a credit line to the material. If material is not included in the article's Creative Commons license and your intended use is not permitted by statutory regulation or exceeds the permitted use, you will need to obtain permission directly from the copyright holder. To view a copy of this license, visit <http://creativecommons.org/licenses/by/4.0/>.

© The Author(s) 2021